

Controlling the Geometry (Janus Balance) of Amphiphilic Colloidal Particles

Shan Jiang and Steve Granick*

Departments of Materials Science and Engineering, Chemistry, and Physics,
University of Illinois, Urbana, Illinois 61801

Received October 20, 2007. In Final Form: November 15, 2007

A simple, generalizable method is described to produce Janus colloidal particles in large quantity with control over their respective hydrophobic and hydrophilic areas (Janus balance) in large quantity. To this end, charged particles adsorb onto the liquid–liquid interface of emulsions of molten wax and water in the presence of surfactants of opposite charge, whose concentration modifies how deeply particles penetrate the oil–water interface, and subsequent surface chemical modification of the resulting colloidosomes is performed after lowering temperature to solidify the wax. Silica particles modified in this way using different amounts of didodecyldimethylammonium bromide (DDAB) display contact angles that vary controllably between 37° and 75°. Janus balance also varies but over a more limited range with control of pH, salt concentration, or the presence of nonionic surfactant (Tween 20 or ethanol). Purity, Janus balance, and colloidosome structure are evaluated by a combination of fluorescence microscopy, flow cytometry, and scanning electron microscopy (SEM). The three-phase contact angle is obtained by observing SEM images of voids left by particles escaped from the surface. Colloidosomes made in the presence of DDAB are markedly improved with respect to the hexagonal close packing, which helps increase the efficiency of the method. Gram-sized quantities of particles are synthesized.

Introduction

A traditional goal in colloid and particle science is to obtain particles whose chemical composition is homogeneous. Not only is this the basis of numerous industrial and other technological applications, but also on the scientific side it is driven by the desire to use colloids to emulate atomic systems where homogeneous chemical makeup of the elements in the system is essential.¹

At the same time, of emerging interest is the idea of obtaining “Janus” particles whose surface chemical composition differs on two sides of the particle. The first Janus particles were synthesized in a laboratory inspired by de Gennes,² who called attention to them in his Nobel Prize address.³ To date, an impressive number of methods have been developed to fabricate Janus particles.^{4–10} This field of experimental study appears now poised to implement the vision of “molecular colloids” whose asymmetric and directional surface interactions induce particles to self-assemble into superstructures.^{11–16} Indeed, the assembly

of larger (non-Brownian) objects has already been implemented.^{17,18} Generalizing this concept, it is natural to also view Janus particles as potential building blocks for novel 3D self-assembled structures.

For these purposes, large amounts of Janus particles are required. In the present study, we build upon a method introduced recently by this laboratory to achieve this.¹⁹ The idea is that at the liquid–liquid interface of emulsified molten wax and water, untreated particles adsorb and are frozen in place when the wax solidifies. The exposed surfaces of the immobilized particles are modified chemically. Finally, wax is dissolved, and the inner surfaces are modified chemically. However, a limitation of the original method is that the relative areas of the two sides of the Janus particle cannot be controlled. If one could achieve control over the relative portions of particles that are rendered hydrophilic and hydrophobic, it would be analogous to controlling the well-known HLB (hydrophilic–lipophilic balance) of classical molecular-sized surfactants.²⁰ For Janus particles, we refer to the balance between hydrophilic and hydrophobic elements as the “Janus balance”.

Careful consideration is worthwhile for the definition of Janus balance. A strict quantitative definition should consider the dimensionless ratio of work to transfer an amphiphilic colloidal particle from the oil–water interface into the oil phase, normalized by the work needed to move it into the water phase, as we have reported.²¹ In the present paper, we simply refer the geometry of the Janus particle to the relative proportion of its hydrophilic and hydrophobic areas.

The aim of this paper is to present a simple, generalizable method to meet the need to control the Janus balance. The method developed here demonstrates that the Janus balance can be controlled over a wide range. The idea is to begin with particle-stabilized emulsions as previously¹⁹ but to vary the three-phase

(1) van Blaaderen, A. *Science* **2003**, *301* (5632), 470–471.
(2) Casagrande, C.; Fabre, P.; Raphael, E.; Veyssie, M. *Europhys. Lett.* **1989**, *9*, 251–255.
(3) de Gennes, P. G. *Rev. Modern Phys.* **1992**, *64*, 645–648.
(4) Perro, A.; Reculusa, S.; Ravaine, S.; Bourgeat-Lami, E. B.; Duguet, E. *J. Mater. Chem.* **2005**, *15*, 3745–3760.
(5) Roh, K. H.; Martin, D. C.; Lahann, J. *Nat. Mater.* **2005**, *4*, 759–763.
(6) Takahara, Y. K.; Ikeda, S.; Ishino, S.; Tachi, K.; Ikeue, K.; Sakata, T.; Hasegawa, T.; Mori, H.; Matsumura, M.; Ohtani, B. *J. Am. Chem. Soc.* **2005**, *127*, 6271–6275.
(7) Cui, J. Q.; Kretzschmar, I. *Langmuir* **2006**, *22*, 8281–8284.
(8) Dendukuri, D.; Hatton, T. A.; Doyle, P. S. *Langmuir* **2007**, *23*, 4669–4674.
(9) Nie, L.; Liu, S. Y.; Shen, W. M.; Chen, D. Y.; Jiang, M. *Angew. Chem., Int. Ed.* **2007**, *46*, 6321–6324.
(10) Pradhan, S.; Xu, L.-P.; Chen, S. *Adv. Funct. Mater.* **2007**, *17*, 2385–2392.
(11) Zhang, Z. L.; Glotzer, S. C. *Nano Lett.* **2004**, *4*, 1407–1413.
(12) De Michele, C.; Gabrielli, S.; Tartaglia, P.; Sciortino, F. *J. Phys. Chem. B* **2006**, *110*, 8064–8079.
(13) van Blaaderen, A. *Nature* **2006**, *439*, 545–546.
(14) Van Workum, K.; Douglas, J. F. *Phys. Rev. E* **2006**, *73*, 031502.
(15) Edwards, E. W.; Wang, D. Y.; Mohwald, H. *Macromol. Chem. Phys.* **2007**, *208*, 439–445.
(16) Glotzer, S. C.; Solomon, M. J. *Nat. Mater.* **2007**, *6*, 557–562.

(17) Terfort, A.; Bowden, N.; Whitesides, G. M. *Nature* **1997**, *386*, 162–164.
(18) Onoe, H.; Matsumoto, K.; Shimoyama, I. *Small* **2007**, *3*, 1383–1389.
(19) Hong, L.; Jiang, S.; Granick, S. *Langmuir* **2006**, *22*, 9495–9499.
(20) Griffin, W. C. *J. Soc. Cosmet. Chem.* **1950**, *1*, 16.
(21) Jiang, S.; Granick, S. *J. Chem. Phys.* **2007**, *127*, 161102.

contact angle of particles at the water–wax interface, as this determines the Janus balance that results after surface chemical modification.

Along with providing an efficient method to produce Janus particles of different Janus balance in large quantity, the simple wax system described here also provides a good opportunity to observe the details of particle self-assembly structure at the liquid–liquid interface. The three-phase contact angle, which normally is hard to measure, can be obtained by observing the SEM images of the voids left by particles escaped from the surface. As will be described below, phase inversion (from oil/water to water/oil) was also observed in the course of varying the concentration of surfactant.

Experimental Section

Chemicals. Monodisperse silica spheres from different vendors were used. Particles larger than 1 μm in diameter were purchased from Tokuyama, Japan, and used as received. Since the particles were synthesized by the Stöber method, the surfaces were fully covered by silanol groups. Particles of 500 nm in diameter were purchased from Fiber Optic Center Inc. Particles of 100 nm in diameter were purchased from Alfa Aesar. These particles were pretreated with Piranha solution in order to fully activate and clean the particle surface. Paraffin waxes of various melting points in the range 55 to 65 $^{\circ}\text{C}$ were purchased from Fisher Scientific and Aldrich. Didodecyltrimethylammonium bromide (DDAB, 98%), (3-aminopropyl)triethoxysilane (APS, 99%), and dichlorodimethylsilane (DCDMS, 99.5%) were purchased from Aldrich.

To produce fluorescent-labeled APS, rhodamine B isothiocyanate (RITC) and fluorescein isothiocyanate isomer (FITC) was attached to APS using a procedure described in the literature.²²

Fabrication of Janus Particles. First, 0.2 g of silica spheres 3 μm in diameter (this amount was decreased as needed when dealing with smaller particles) were dispersed in 0.5 g of paraffin wax at 75 $^{\circ}\text{C}$ by stirring and then mixed with 5 mL of DDAB dissolved in water. Emulsions were produced using magnetic stirring at 1500 rpm for 15 min and then cooled to room temperature, at which paraffin wax is solid. Deionized water was used to wash the wax emulsions multiple times to remove unattached or weakly attached particles from the aqueous solution. After completely drying the emulsion under vacuum for 5 h, the resulting exposed surfaces of particles attached to the emulsions were allowed to react chemically with 2 mM of DCDMS in methanol solution for 20 min. A 2 mM concentration of triethylamine was added to speed up the reaction.

An important technical detail is that the act of adding surfactant caused the surrounding wax to be more easily dissolved by solvent. Two methods were developed to prevent this. One was to perform silanization below room temperature (0 $^{\circ}\text{C}$). Another route to solve this problem was to use wax with higher melting point. Both methods were found to be effective.

After the reaction, the colloidosomes were filtered to remove the excess silane and the free particles. To release the modified silica particles from colloidosomes, the wax was dissolved in chloroform at room temperature. Particles (~ 0.2 g) were washed with 300 mL of chloroform and 1200 mL of ethanol and then redispersed into ethanol.

Removal of DDAB from the particle surfaces was easily accomplished by rinsing. This we confirmed by two easy control experiments. First, a silicon wafer was immersed in high concentration DDAB solution, at which point the water contact angle for the DDAB-covered wafer was $\sim 85^{\circ}$. After the wafer was simply dipped into ethanol, water was observed to fully wet the wafer. Next, to check the efficacy of the washing on particles, control experiments were also carried out on particle-stabilized emulsions. The particles on the colloidosomes before modification were collected and washed using the same washing protocol mentioned above and then used to stabilize a water–toluene emulsion. The emulsion stability was

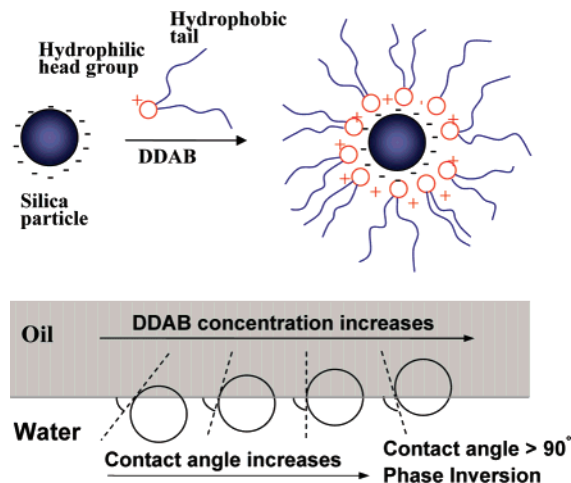


Figure 1. Schematic representation of the experimental strategy. Particles adsorb to the water–oil interface of emulsions, and the distance that the particle penetrates the respective phases determines a contact angle depicted by the dotted line. For silica particles, the cationic surfactant DDAB adsorbs strongly and renders the particle more hydrophobic, causing them to penetrate more deeply into the oil phase. Changing the surfactant concentration systematically varies the particle hydrophobicity, which results in systematic changes of the contact angle. Particles with different Janus balance can be obtained simply by controlling the amount of surfactant. The DDAB is rinsed off later using ethanol.

found to be indistinguishable from that of this same emulsion stabilized using bare hydrophilic silica particles.

Fluorescence imaging was applied to check whether a Janus geometry was successfully produced. The exposed area of the particles on the colloidosomes was modified by DCDMS first, particles were then released, and finally fluorescent-labeled APS was allowed to react with the wax-protected part. A 0.1 mL amount of APS-RITC or APS-FITC dye solution was added to 5 mL of particle ethanol suspension. The reaction proceeded for 30 min under ultrasonication.

Characterization. Scanning electron microscopy, SEM (JEOL6060 LV), was used to image the colloidosomes. Prior to imaging, a thin layer (15 nm) of gold was evaporated onto them to render them electrically conductive, avoiding surface charging under the electron beam. By measuring the size of voids left by particles that escaped from the wax surface during the processing steps, the three-phase contact angle was determined.

For epi-fluorescence imaging of the Janus geometry, the optics employed a Zeiss Axiovert 200 microscope. A Nd:YAG laser (532 nm) was focused at the back focal point of a 63 \times air objective. The fluorescence images were collected using this same objective and recorded using an electron multiplying CCD camera (Andor iXon) after filtering out light from the excitation laser. Images of particle rotation were recorded with an exposure time of 0.05 s for 800 frames. APS-RITC labeled particles were used in this experiment.

For flow cytometry measurement of the Janus geometry, we employed the commercial BD LSR II system located in the Carver Biotechnology Center at the University of Illinois. In a typical experiment, particles were dispersed in aqueous solution at the concentration of ~ 10 mg/mL. The small fraction of dimers formed by self-assembly was filtered out by the software provided with the equipment and was not included in the analysis. APS-FITC labeled particles were used in this experiment to give fluorescence under laser excitation of 488 nm.

Results and Discussion

The strategy of these experiments is shown schematically in Figure 1. When particles adsorb to the liquid–liquid (usually water–oil) interface, as is known to happen ubiquitously and forms the basis of forming colloidosomes,²³ the distance that particles penetrate into the oil determines the respective areas

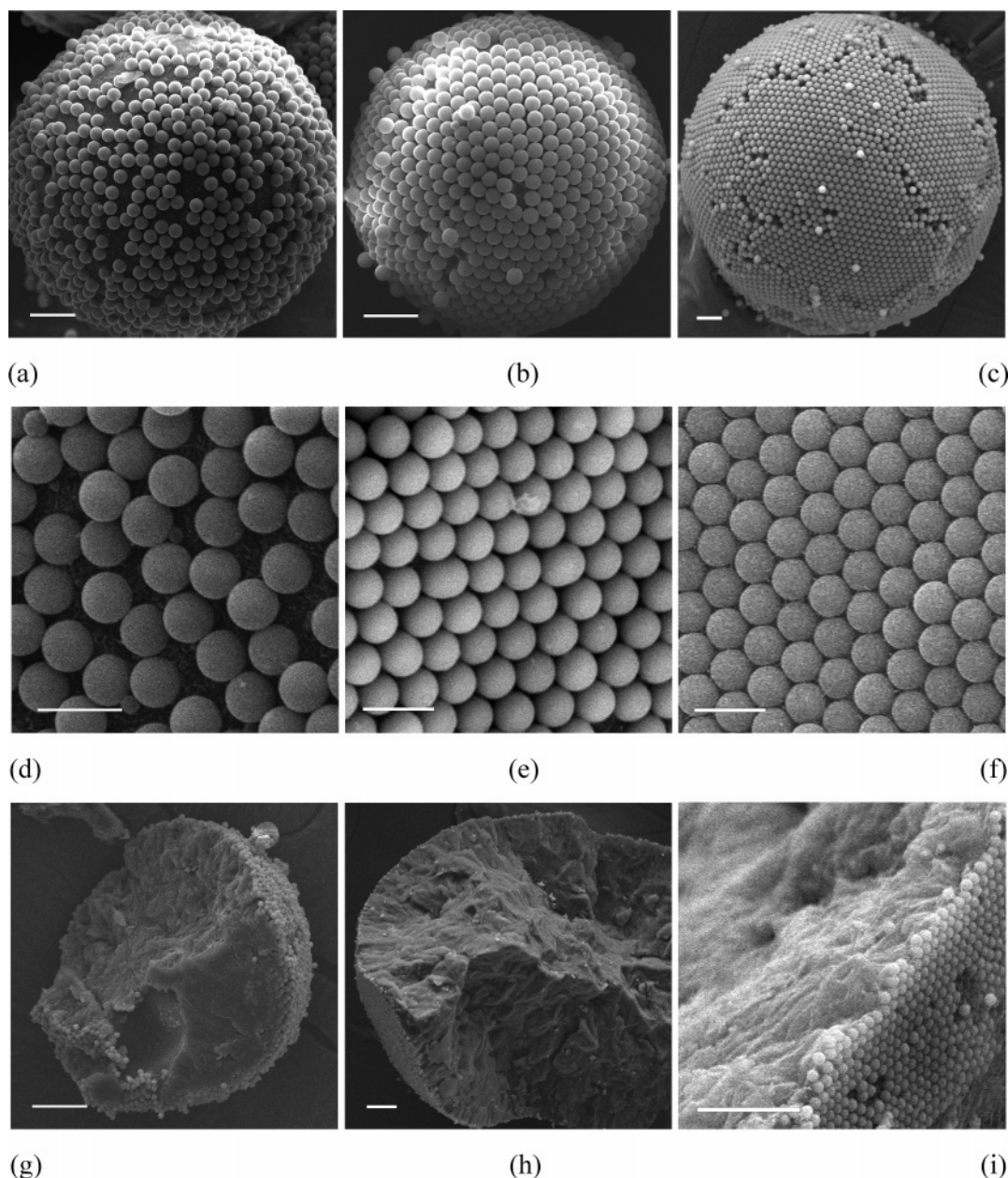


Figure 2. SEM micrographs illustrating colloidosome structure. Panels a, b, and c show that as the surfactant concentration increases, silica particles became more close packed and better ordered. The concentrations of DDAB relative to water used to form the colloidosome are 0, 20, 60 $\text{mg}\cdot\text{L}^{-1}$ in panels a, b, and c, respectively. In these images, very few particles stick on top of the colloidosome monolayer owing to imperfect washing or detachment of particles during the SEM sample preparation. Panels d, e, and f show magnified images of samples from a, b, and c, respectively. Panels g, h, and i display the insides of representative colloidosomes. No unattached particles are visible within the wax phase, indicating that almost all the unattached particles segregated to the water phase. Here the images are cross-sections of colloidosomes after squeezing them between two glass slides to break them apart. Particles in all the images have $3\ \mu\text{m}$ diameter, except in image i, where diameter is $500\ \text{nm}$. In panels a, b, and c, scale bar = $10\ \mu\text{m}$; in panels d, e, f, and i, scale bar = $5\ \mu\text{m}$; in panels g and h, scale bar = $20\ \mu\text{m}$.

of hydrophilic or hydrophobic patches resulting from subsequent surface chemical modification of the portions that dwell on the two sides of the interface. The distance penetrated into the oil phase increases if the particle becomes increasingly hydrophobic by allowing surfactant of opposite charge to adsorb. In this way the contact angle drawn in the figure increases. Adsorption of cationic surfactant is favored because the silica particle surface is negatively charged at the pH used in these experiments. We now turn to specific results from pursuing this strategy.

Colloidosome Structure. Structures obtained from extensive SEM measurements are illustrated in Figure 2. The main point is that a striking improvement in the close and regular particle packing resulted from having cationic surfactant present when silica particles assembled at the water–oil interface. This greatly improves the efficiency of the adsorption of the particles. Here, panels a–c compare zero, intermediate, and high surfactant concentration, while panels d–f present magnified views of the same samples.

After these colloidosomes were broken apart, cross-sections of the colloidosome interiors (panels g–i) reveal no visible

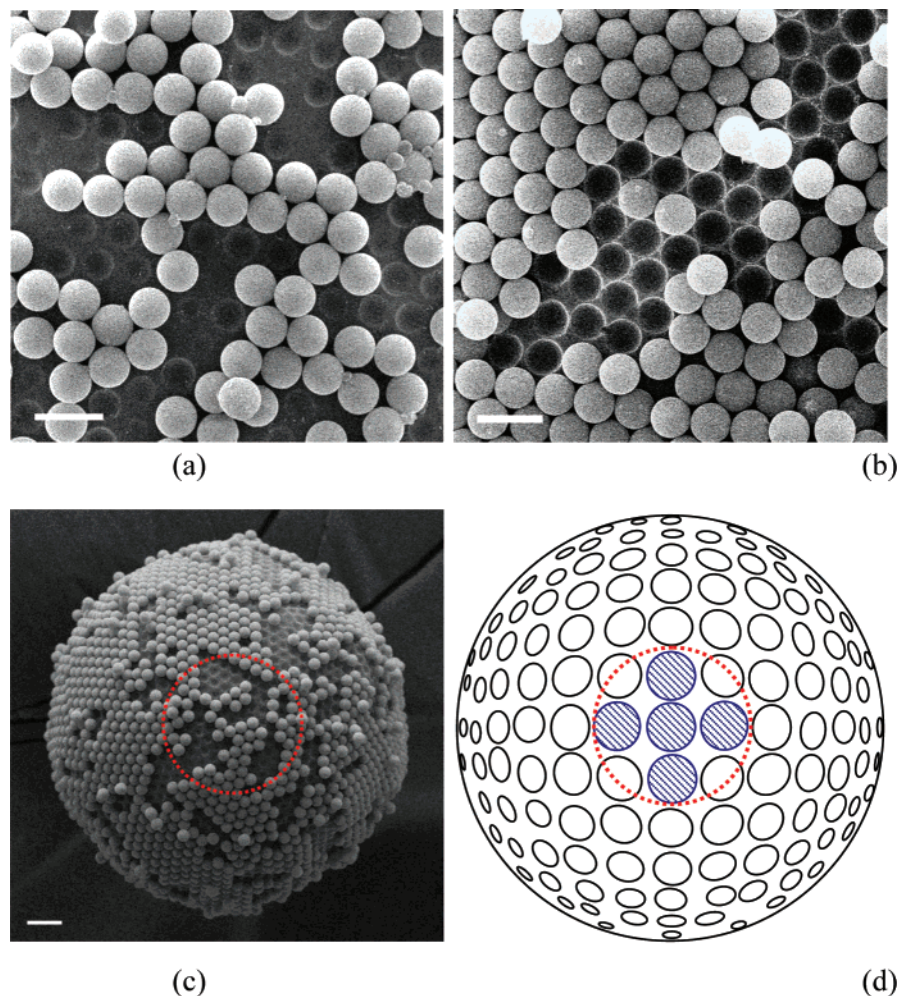


Figure 3. Contact angle was quantified from analysis of SEM images of voids left behind when particles are rinsed away from the wax surface by ethanol. Panels a and b illustrate the ubiquity of voids. Panel c illustrates the complication of curvature. Panel d illustrates schematically the approach taken in this paper for subsequent analysis of SEM images to deduce the contact angle: the electron beam was focused at a right angle to the top of the sample. Particle size is $3\ \mu\text{m}$. In panels a and b, scale bar = $5\ \mu\text{m}$; in panel c, scale bar = $10\ \mu\text{m}$.

unattached particles. So the second key conclusion is that unattached particles segregated to the water phase only. However, the fraction of unattached particles was small. From simply weighing the dried emulsions, we estimated more than 90% of particles to reside at the interfaces.

How can it be explained that close-packed structures resulted only in the presence of surfactant? Two factors should be taken into account. One is that adsorption energy increases as contact angle increases. It has been calculated that the adsorption energy is the highest at 90° contact angle.²⁴ Another factor is that the adsorption of cationic surfactant neutralizes negative charges on the silica surface, weakening electrostatic repulsion between neighboring particles. At the same time, the hydrophobized particle surfaces (by adsorbed surfactant) may attract one another through the water phase.

However, reflection shows that other factors come into play, factors whose definitive elucidation is outside the scope of this paper. One complexity is how to consider the charge–charge interactions between neighboring particles;²⁵ in this situation, some charges on the particles reside in the water phase but other charges reside in the oil phase. It is also hard to know how many surfactant molecules may have been adsorbed onto the adsorbed

colloidal particles, since surfactant may distribute unevenly along the water–wax interface and also partition between the water and wax phases. Furthermore, it is plausible to imagine a scenario in which surfactant molecules partition preferentially to the particle–oil interface to accommodate more easily the long hydrophobic tail. Selective partitioning of this kind, putting more surfactant on the oil side, would itself tend to produce a Janus particle, even before the subsequent chemical modification step. Though further experiments are desirable to resolve these interesting issues, the main point of the data in Figure 2 is to show the beneficial influence of surfactant in achieving close-packed colloidal assemblies on these emulsion surfaces, free of unattached particles on their insides.

Method To Quantify the Contact Angle on a Janus Particle.

This study required quantification of the contact angle when a colloid particle sits at an interface (Figure 1), but in the beginning how to quantify contact angle on a sphere was not clear. A solution emerged from inspecting SEM micrographs of the voids left in the wax after particles were removed during processing steps. This information, the imprint of how much particle was immersed in the wax (oil) phase, contains what is needed. Figure 3 shows the basis of these calculations. Panels a and b, images of voids in wax, illustrate the raw data, but images taken at an oblique angle are difficult to quantify correctly owing to curvature (panel

(24) Binks, B. P.; Fletcher, P. D. I. *Langmuir* **2001**, *17*, 4708–4710.

(25) Horozov, T. S.; Aveyard, R.; Clint, J. H.; Binks, B. P. *Langmuir* **2003**, *19*, 2822–2829.

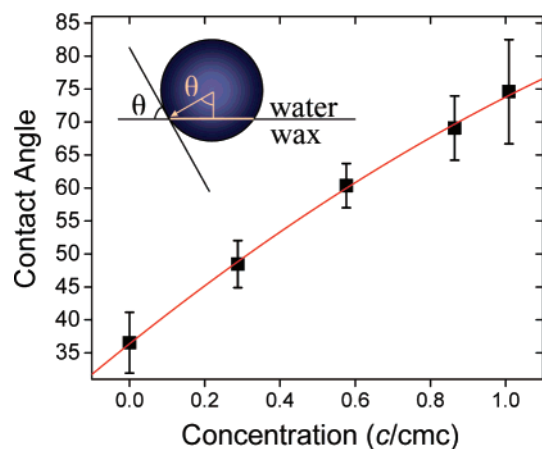


Figure 4. Contact angle of Janus colloids formed using DDAB surfactant of various concentrations during the preparation of colloidosomes, plotted as a function of DDAB concentration c normalized by cmc (69.4 mg L^{-1}) of DDAB. Inset is a schematic representation of the contact angle. Line through the points is a guide to the eye. Error bars are the standard deviation of more than 30 measurements. Phase inversion concentration, from O/W to W/O, was observed at higher concentrations than indicated here.

c). For quantitative analysis, these voids should reside at right angles to the electron beam (panel d).

The effect of curvature on the contact angle has been investigated theoretically²⁶ with the conclusion that the equilibrium contact angle does not depend on the curvature of the interface in reference. In order to confirm this, we carried out the contact measurement on two individual wax colloidosomes, $\sim 20 \mu\text{m}$ and $\sim 100 \mu\text{m}$ diameter. Since the particles on $20 \mu\text{m}$ colloidosomes were fewer, the statistics of measurement were worse. The contact angle was the same within experimental uncertainty: $46.8 \pm 1.9^\circ$ ($20 \mu\text{m}$ wax colloidosome) and $48.5 \pm 3.6^\circ$ ($100 \mu\text{m}$ colloidosome). The quoted uncertainty is the standard deviation from 12 and 40 data points in the two respective cases, more data points in the latter case reflecting the larger size of the colloidosome. These considerations imply that contact angle is relatively homogeneous, even when the size distribution of the emulsion droplet is broad.

How Contact Angle of Janus Particles Depends on Surfactant Concentration. In Figure 4, the contact angle of Janus particles is plotted against DDAB concentration during the preparation of colloidosomes. One sees that the contact angle

more than doubled, from 37° without surfactant, to 75° at the highest concentration. Inspection of this figure shows that error bars in the data became larger when approaching 75° . The reason is not that void size became more heterogeneous, but simply that the sinusoidal relationship between the three phase contact angle and the size of the voids increases uncertainty owing to the nature of the underlying mathematical function to make this connection.

It is worth mentioning some other phenomena we observed during these processes, although to pursue the details of them falls beyond the scope of this study. As the concentration of DDAB approaches the point of phase inversion, the emulsion droplet size increases and the emulsion droplets are observed to adopt nonspherical shapes as shown in the SEM images in Figure 5 (panel a). The particle monolayer at the water–wax interface often displays surface facets (panel b) and ripples (panel c). This same behavior was observed using several different waxes and particles with different sizes, so appears to be general. Similar phenomena have also been reported from several other groups recently for water–oil emulsions or air–water foams stabilized by particles with different hydrophobicity.^{27,28} When the surfactant concentration was raised even higher, the phenomenon of phase inversion intervened, from oil/water to water/oil emulsion.

The main point here was to demonstrate that this method to modify the three-phase contact angle was effective, more so than other approaches that we also attempted. We speculate that the different levels of surfactant concentration altered the bending rigidity of the wax droplet, in this way changing the emulsion droplet size. However, detailed examination of this point falls beyond the scope of this paper.

Other Methods To Change the Contact Angle. Changes of Janus balance could also be effected, but over a more limited range, by control of pH, salt concentration (NaCl), or the presence of nonionic surfactant (Tween 20 or ethanol), as shown in Figure 6. Panels a and b show that adding salt or ethanol to the water phase diminished the three-phase contact angle, but moderately. It may be that these substances reduced the surface tension between wax and water. Consistent with this argument, SEM images of the resulting colloidosomes (not shown) revealed that many particles were washed off during cleansing procedures, presumably because the three-phase contact angle was too low for the wax surface to hold the silica particles tightly. It was also observed from SEM images that at the highest salt concentrations, particles on the colloidosomes became better close-packed. This

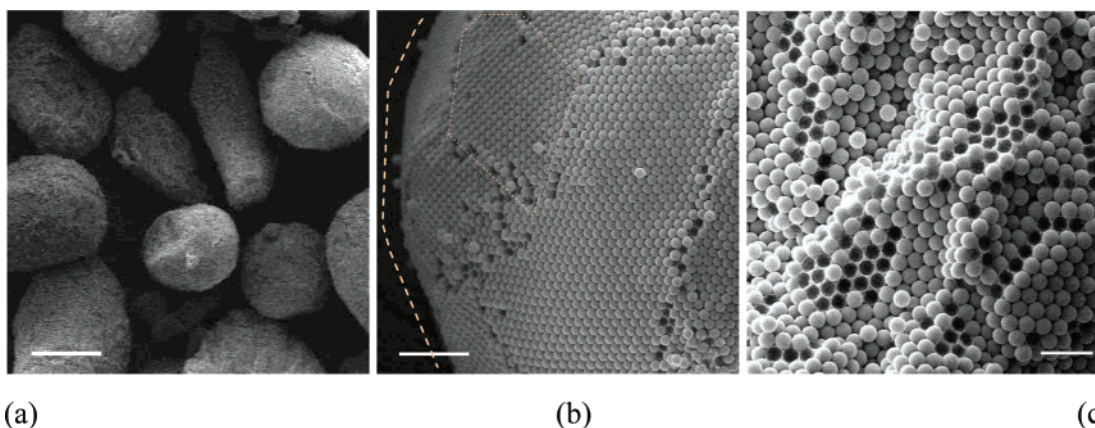


Figure 5. SEM images of colloidosome shape and structure for a system prepared at a DDAB surfactant concentration (70 mg/mL) close to the point of phase inversion. Panel a illustrates the common nonspherical shape of emulsion droplets. Panel b illustrates the common observation of surface facets, highlighted in this image by the dotted lines. Panel c shows the common observation of ripples on the surface. The voids from detached particles exposed wax underneath, which indicates that particles formed a monolayer. Particle size is $3 \mu\text{m}$. In panel a, scale bar = $100 \mu\text{m}$; in panel b, scale bar = $20 \mu\text{m}$; in panel c, scale bar = $10 \mu\text{m}$.

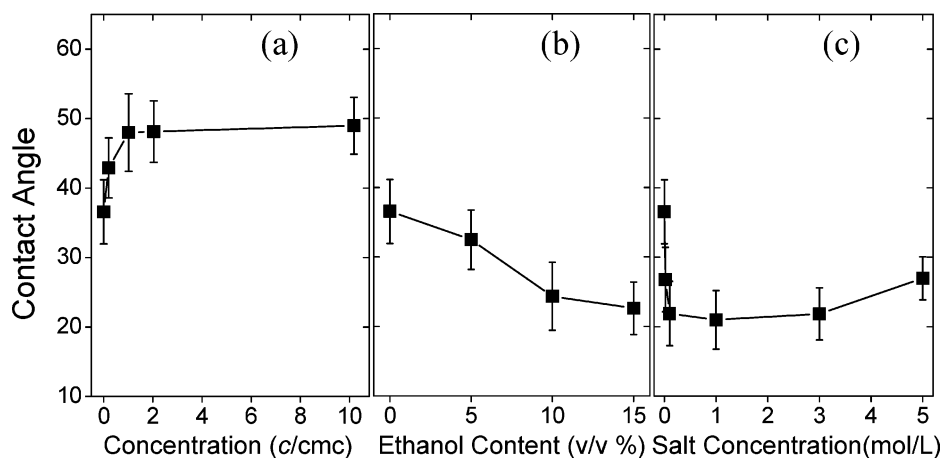


Figure 6. Contact angle is plotted versus (a) Tween 20 concentration c relative to water phase; here c is normalized by cmc ($98.2 \text{ mg}\cdot\text{L}^{-1}$) of Tween 20, (b) ethanol volume fraction relative to water phase, and (c) salt (NaCl) molar concentration relative to water phase. Error bars are the standard deviation of more than 30 measurements.

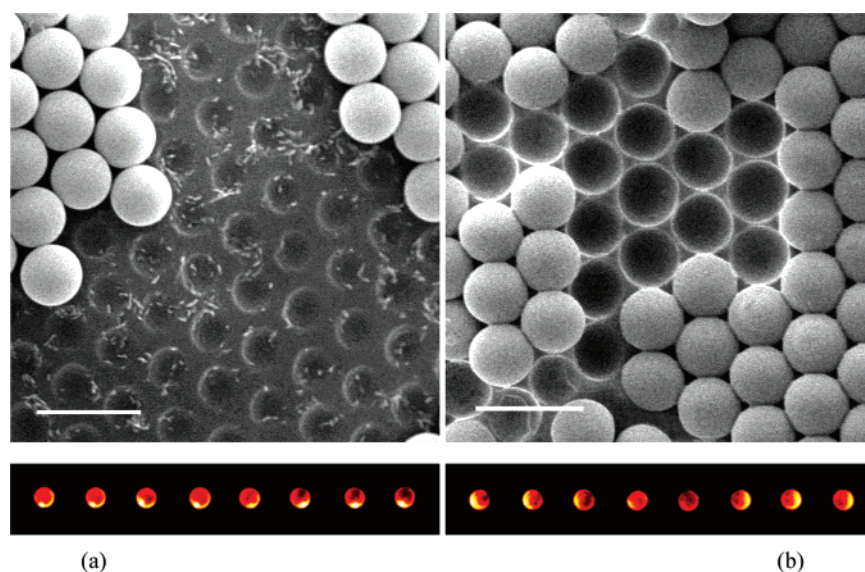


Figure 7. Comparison of SEM images of particles with different geometry (top panels) and corresponding epi-fluorescence images in water after fluorescence labeling of the protected surface as described in the text. The epi-fluorescence images show the Janus character of the particles. The fluorescence illuminated area agrees well with the size of the holes shown in the SEM images. DDAB concentration during the preparation is (a) 20 mg L^{-1} ; (b) 60 mg L^{-1} . Particle size is $3 \mu\text{m}$, scale bar = $5 \mu\text{m}$.

is understandable since high salt concentration of course screened electrostatic repulsion between silica particles.

In a different approach, we also changed the pH when forming the colloidosomes. At pH = 3 (near the isoelectric point of silanol groups), SEM micrographs showed the wax to be almost fully covered by close-packed silica structures (not shown), as expected for minimal electrostatic repulsion. The same behavior was observed by using either HCl or H₂SO₄ as the agent to tune the pH. However, the change of contact angle over pH ranges from 1 to 10 is small ($\sim 10^\circ$).

Another interesting thought about how to change the contact angle is to consider initially dispersing particles in the water phase instead of the wax. The difference in advancing and receding angle may then produce different contact angles when particles adsorb. However, this will not give the systematic changes demonstrated above using DDAB surfactant. Another point worth mentioning is that though hydrophilic particles do not disperse

well in the wax phase initially, the SEM images shown above of rather perfect particle monolayers on the colloidosomes indicate that their initial aggregation in the wax phase did not seem to degrade efficient formation of the particle monolayer at the interface.

Validation of the Janus Geometry. Suspicious by nature, we also sought direct validation that these synthesis methods did produce Janus particles. In the first approach, once particles were released from wax after their exposed area was rendered hydrophobic, the polar side was made fluorescent by reaction with fluorescent-labeled APS (aminopropylsilane). Epi-fluorescence imaging (Figure 7, bottom) then revealed directly the Janus geometry of the resulting particles (SEM images in Figure 7, top). Complications emerged, however, when we sought to quantify these and similar images. The first difficulty is that silica particles of micron size are transparent but not completely so; therefore, the fluorescence intensity depends on which side of a Janus particle faces the excitation light source and the detector. Second, some dye was found to physically adsorb onto the hydrophobic side of the particles, smearing the comparison. Third, the particle's rotation owing to Brownian motion also smeared

(26) Komura, S.; Hirose, Y.; Nonomura, Y. *J. Chem. Phys.* **2006**, *124*, 241104.
 (27) Kim, S. H.; Heo, C. J.; Lee, S. Y.; Yi, G. R.; Yang, S. M. *Chem. Mater.* **2007**, *19*, 4751–4760.
 (28) Subramaniam, A. B.; Abkarian, M.; Mahadevan, L.; Stone, H. A. *Nature* **2005**, *438*, 930–930.

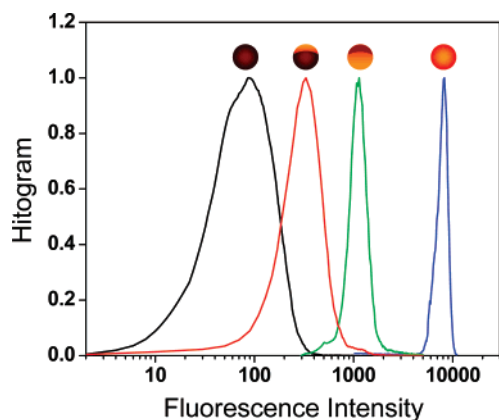


Figure 8. Flow cytometry experiments, comparing the histogram of fluorescence intensity for two samples of Janus particles and two samples of homogeneous particles. The single peak observed in all cases reflects purity of the samples. In the schematic representation that identifies particles above each histogram, the dark areas represent the area with lower fluorescence intensity. From left to right, the samples are (1) homogeneous particles rendered hydrophobic by reaction with dichlorodimethylsilane (DCDMS) and then reacted with FITC-labeled aminopropylsilane, APS-FITC, (2) Janus particles synthesized first by rendering hydrophobic the exposed areas on each colloidosome by reaction with DCDMS and then allowing the inside areas to react with APS-FITC, (3) Janus particles synthesized by allowing only the exposed areas on each colloidosome to react with APS-FITC, and (4) homogeneous particles, prepared by allowing the entire surface area to react with APS-FITC. Particle size is $3 \mu\text{m}$.

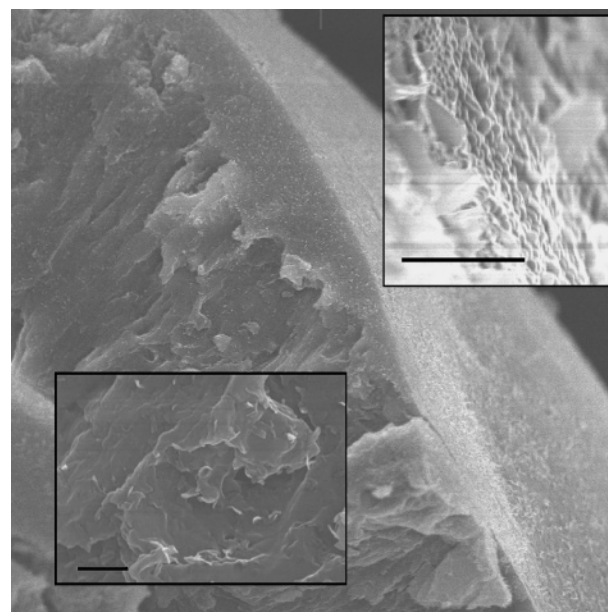
optical images. In spite of these difficulties regarding quantification, it is clear qualitatively that the higher the three-phase contact angle, the higher the fluorescence intensity. This is as expected since the fluorescent dye adsorbed preferentially on the polar regions of these colloids.

The technique of flow cytometry, which compares the fluorescence intensity of cells or particles one by one, provided additional characterization of these Janus particles, allowing us not only to differentiate between particles of different Janus balance but also to evaluate their purity. Figure 8 compares histograms of the fluorescence intensity for two samples of Janus particles and two samples of particles that were labeled homogeneously with fluorescent dye as described in the figure caption.

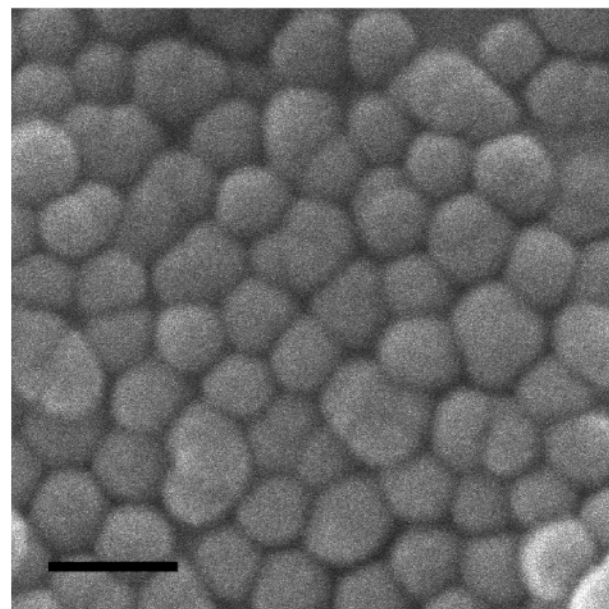
The fact that a single peak was observed for Janus particles shows that the particles produced by this method were pure, with no detectable homogeneous hydrophobic or hydrophilic particles. In addition, the data in Figure 8 show that the larger the portion of the particle that is fluorescently labeled, the fluorescence intensity is higher. However, to date we have not found a simple linear relation between fluorescent area and fluorescence intensity. Besides the complications mentioned in the quantification of epi-fluorescence images, other factors that may influence fluorescence intensity are the transparency and rotation of silica particles such that the experiment is sensitive to which projection of the Janus geometry faces the excitation laser and the detector, even though the particle makeup is the same.

Smaller Particles. Silica particles as small as 500 nm in diameter have also been used successfully to synthesize Janus particles. The SEM images in Figure 9 show that silica particles of 100 nm in diameter also form colloidosomes of high quality on these wax emulsions. Therefore, the methods described in this paper also apply to sub-micron-sized particles by rational extension.

Prospects. We anticipate the methods described in this paper to generalize to other particles than the silica spheres studied here. One of the main conclusions is to demonstrate that for



(a)



(b)

Figure 9. SEM images of colloidosomes stabilized by 100 nm silica particles with 20 mg/L DDAB. Panel a shows that the interior of the wax emulsion contains no particles; all particles reside at the interface. The inset, a magnified portion of the main image, confirms this. Panel b shows the close-packed structure of particles on the wax surface. Particles are extremely close packed due to the heterogeneity of particles from the vendor. In panel a, scale bar = $1 \mu\text{m}$; in panel b, scale bar = 200 nm.

silica particles (negative charge in water), the most effective modification of Janus balance is predicated on allowing them to coadsorb onto colloidosomes in the presence of surfactant with opposite charge, probably because these surfactants adsorb on particles most strongly while accordingly modifying their hydrophobicity. By the same logic, it is natural to expect that coadsorption of anionic surfactants will be effective when it is desirable to modify the Janus balance of cationic particles.

This method can be simply extended to synthesize Janus particles with different charges on the two sides, by using positive charged silane molecules, e.g., (3-aminopropyl)triethoxysilane (APS), to modify the exposed area of the silica particles on the

emulsion. The amine group can act as the reactive site for even further modification. Also, this method can be applied to synthesize stand-alone particle colloidosomes by cross-linking the particles on the emulsion surface. The methodologies described in this paper are anticipated to also apply for the surface chemical modification and characterization of particles with other shape, for example to rod-shaped particles.

Looking to the future, we expect the Janus balance to determine many properties of Janus particles, such as their self-assembly behavior and their ability to stabilize water–oil emulsions and water–air foams. Experiments in these directions are in progress and will be reported elsewhere.

Acknowledgment. This work was supported by the U.S. Department of Energy, Division of Materials Science, under Award No. DEFG02-91ER45439 through the Frederick Seitz Materials Research Laboratory at the University of Illinois at Urbana–Champaign. For instrumental support, we acknowledge the Donors of the Petroleum Research Fund, administered by the American Chemical Society, # 45523-AC7. We also want to thank Prof. Bernard P. Binks at the University of Hull, U.K., for useful discussion, and Mr. Bo Wang for performing the characterization experiments using flow cytometry.

LA703274A